

Possible Common Origin of the Top Forward-backward Asymmetry and the CDF Dijet Resonance

Dong-Won Jung^{a,b}, P. Ko^c and Jae Sik Lee^{a,b}

^a*Department of Physics, National Tsing Hua University, Hsinchu, Taiwan 300*

^b*Physics Division, National Center for Theoretical Sciences, Hsinchu, Taiwan 300*

^c*School of Physics, KIAS, Seoul 130-722, Korea*

ABSTRACT

A color-singlet neutral vector boson is considered as a possible common origin of the top forward-backward asymmetry and the CDF dijet resonance. We identify chiral and flavor structures of the couplings of this new vector boson to the standard model quarks for which one could accommodate both data. We also demonstrate that non-vanishing observables involving longitudinal top polarizations can provide useful criteria for the possible existence of parity violating new physics in the $q\bar{q} \rightarrow t\bar{t}$ process, and discrimination between the flavor-conserving and flavor-violating cases.

1 Introduction

Top forward-backward (FB) asymmetry has been exciting subject, since the data showed deviation from the SM predictions at the level of 2-3 σ [1]. There have been a lot of study on this subject. It is still premature what kind of new physics could be responsible for the observed deviations. If the FB asymmetry can be measured as functions of $M_{t\bar{t}}$ and $\Delta y \equiv y_t - y_{\bar{t}}$ with nontrivial structures in them, it could provide more informations on the underlying physics. Also the measurements of the FB spin-spin correlations in the $t\bar{t}$ production and (anti)top longitudinal polarization could provide more informations on the underlying physics behind the observed top FB asymmetry [2, 3].

Recently the CDF Collaboration reported another interesting data on Wjj channel [4]. The result is that a broad peak in the 120 – 160 GeV dijet invariant mass range, with the estimated production cross section ~ 4 pb. There is no evidence that these dijets are b -flavored, and no clear resonance structure in Wjj invariant mass spectrum. A number of papers stimulated by this peak have appeared discussing it in various contexts [5–23]. The D0 Collaboration also reported the study of the dijet invariant mass distribution in $p\bar{p} \rightarrow W(\rightarrow l\nu) + jj$ final states [24]. They found no evidence for anomalous resonant dijet production and set a 95 % C.L. limit of 1.9 pb on the cross section for the dijet invariant mass $m_{jj} = 145$ GeV. In this work, without clear understanding of the discrepancy between the two experiments, we postulate a new particle with the production cross section of 1 – 4 pb at the Tevatron. We further assume that it couples dominantly to the quarks in order to evade strong constraints from Drell Yan process.

It would be interesting to ask if one can explain both top FB asymmetry and the dijet resonance in the Wjj channel by introducing a single new particle. It is our purpose to answer this question using a neutral color-singlet vector boson V_μ , assuming the CDF dijet peak is due to $p\bar{p} \rightarrow WV \rightarrow (l\nu)(jj)$. Let us consider the following New Physics (NP) interactions of V_μ :

$$\mathcal{L}_{\text{NP}} = -g_s \sum_{q=u,d,t} \bar{q} \gamma^\mu (g_L^q P_L + g_R^q P_R) q V_\mu - [g_s \bar{u} \gamma^\mu (\tilde{g}_L^t P_L + \tilde{g}_R^t P_R) t V_\mu + h.c.] . \quad (1)$$

The first and second terms describe the flavor-conserving (FC) and flavor-violating (FV) interactions, respectively. We are including the interactions of V_μ with the first-generation quarks and top quarks, since our interest is in $p\bar{p} \rightarrow t\bar{t}$, WV . We are using the strong coupling constant g_s for the overall normalization of the FC $g_{L,R}^q$ and FV $\tilde{g}_{L,R}^t$ couplings for consistency with the model-independent studies of the Tevatron forward-backward asymmetry of top quark (A_{FB}) [2, 3].

Within this framework, we study hadroproductions of WV and V as well as $t\bar{t}$ production and the top FB asymmetry at the Tevatron, and identify the chiral and the flavor structures of couplings that can accommodate both top FB asymmetry and the CDF dijet excess.

2 Hadroproductions of WV and V

The V production associated with W^\pm at hadron colliders occurs via the exchanges of the u , d , and t quarks. We denote the WV production cross section as the sum

$$\sigma_{LO}(\text{had}_1 \text{had}_2 \rightarrow W^- V) = (g_L^u)^2 \sigma_L^u + (g_L^d)^2 \sigma_L^d + (g_L^u g_L^d) \sigma_L^{ud} + |\tilde{g}_L^t|^2 \sigma_L^t + |\tilde{g}_R^t|^2 \sigma_R^t, \quad (2)$$

where

$$\begin{aligned} \sigma_{L,R}^X &= \int_{\sqrt{\hat{s}_{\min}}}^{\sqrt{\hat{s}_{\max}}} d\sqrt{\hat{s}} \int_{\hat{t}_{\min}}^{\hat{t}_{\max}} d\hat{t} \int_{\tau}^1 dx \\ &\times \left[\frac{\tau}{x} f_{\text{had}_1}^D(x, Q_F) f_{\text{had}_2}^{\bar{u}}\left(\frac{\tau}{x}, Q_F\right) + \frac{\tau}{x} f_{\text{had}_1}^{\bar{u}}(x, Q_F) f_{\text{had}_2}^D\left(\frac{\tau}{x}, Q_F\right) \right] \left(\frac{2}{\sqrt{\hat{s}}} \frac{d\hat{\sigma}_{L,R}^X}{d\hat{t}} \right) \end{aligned} \quad (3)$$

where $(X, D) = (u, d), (d, d), (ud, d), (t, b)$ and $\tau = \hat{s}/s$ with s being the centre-of-mass the colliding hadrons. And $\hat{s} = (p_1 + p_2)^2 = (k_1 + k_2)^2$, $\hat{t} = (p_1 - k_1)^2 = (k_2 - p_2)^2$, and $\hat{u} = (p_1 - k_2)^2 = (k_1 - p_2)^2$ with p_1 and p_2 for the momenta of the initial D and \bar{u} quarks, respectively, and k_1 and k_2 for those of the outgoing W^- and V vector bosons, respectively. The symbol $f_{\text{had}_i}^u(x, Q_F)$, for example, is for the u -quark distribution function in the hadron had_i . The kinematic range of \hat{t} is given by

$$\hat{t}_{\max, \min} = \frac{1}{2} (m_V^2 + m_W^2 - \hat{s}) \pm \frac{\hat{s}}{2} \lambda^{1/2} \quad (4)$$

with $\lambda = 1 + (m_V^2/\hat{s} - m_W^2/\hat{s})^2 - 2m_V^2/\hat{s} - 2m_W^2/\hat{s}$. The range of the variable \hat{s} can be determined by requiring $0 < \lambda < 1$ and $x > \tau$. Also note the relation $\hat{s} + \hat{t} + \hat{u} = m_V^2 + m_W^2$. The partonic-level cross sections are given by

$$\begin{aligned} \frac{d\hat{\sigma}_L^u}{d\hat{t}} &= \frac{\pi\alpha\alpha_S}{6s_W^2\hat{s}^2} \frac{(\hat{u}\hat{t} - m_V^2 m_W^2) + \hat{t}^2 E(\hat{s}, \hat{t}, \hat{u})}{\hat{t}^2}, \\ \frac{d\hat{\sigma}_L^d}{d\hat{t}} &= \frac{\pi\alpha\alpha_S}{6s_W^2\hat{s}^2} \frac{(\hat{u}\hat{t} - m_V^2 m_W^2) + \hat{u}^2 E(\hat{s}, \hat{t}, \hat{u})}{\hat{u}^2}, \\ \frac{d\hat{\sigma}_L^{ud}}{d\hat{t}} &= \frac{\pi\alpha\alpha_S}{6s_W^2\hat{s}^2} \left[2\hat{s} \frac{m_V^2 + m_W^2}{\hat{u}\hat{t}} - 2E(\hat{s}, \hat{t}, \hat{u}) \right], \\ \frac{d\hat{\sigma}_L^t}{d\hat{t}} &= \frac{\pi\alpha\alpha_S}{6s_W^2\hat{s}^2} \frac{(\hat{u}\hat{t} - m_V^2 m_W^2) + \hat{t}^2 E(\hat{s}, \hat{t}, \hat{u})}{|\hat{t} - m_t^2 + im_t\Gamma_t|^2}, \\ \frac{d\hat{\sigma}_R^t}{d\hat{t}} &= \frac{\pi\alpha\alpha_S}{6s_W^2\hat{s}^2} \frac{m_t^2 [\hat{s} + \hat{t}F(\hat{s}, \hat{t}, \hat{u})]}{|\hat{t} - m_t^2 + im_t\Gamma_t|^2}, \end{aligned} \quad (5)$$

where

$$\begin{aligned} E(\hat{s}, \hat{t}, \hat{u}) &= \frac{1}{4} \left(\frac{\hat{u}\hat{t}}{m_V^2 m_W^2} - 1 \right) + \frac{1}{2} \frac{(m_V^2 + m_W^2) \hat{s}}{m_V^2 m_W^2} \\ F(\hat{s}, \hat{t}, \hat{u}) &= \frac{\hat{s}\hat{t}}{4m_V^2 m_W^2} + \frac{1}{2} \frac{(m_V^2 + m_W^2)(\hat{u}\hat{t} - m_V^2 m_W^2)}{m_V^2 m_W^2 \hat{t}} \end{aligned} \quad (6)$$

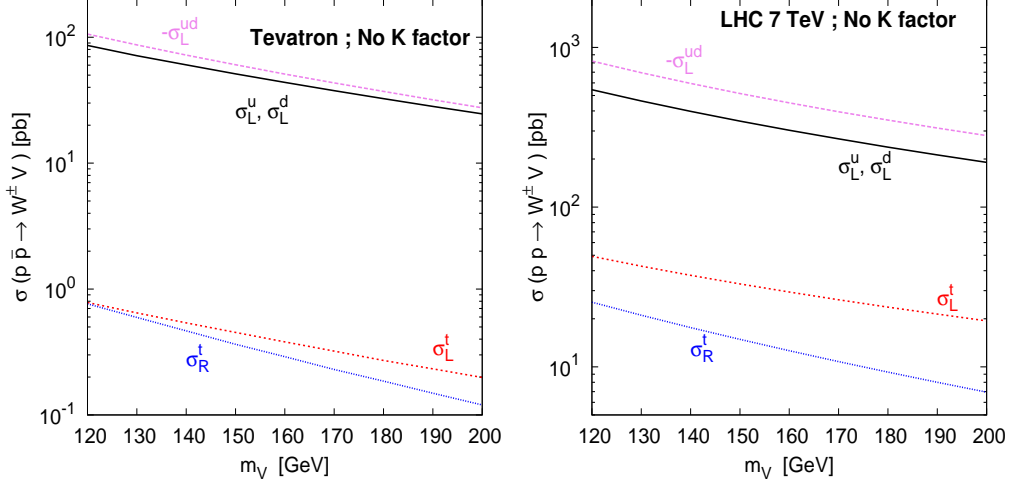


Figure 1: The cross sections σ_L^u , σ_L^d , $-\sigma_L^{ud}$, and $\sigma_{L,R}^t$ as functions of m_V for $\sigma_{LO}(p\bar{p} \rightarrow W^\pm V)$ at the Tevatron (left) and at the LHC with 7 TeV (right).

We verified our expressions agree with those given in Ref. [25] for $\hat{\sigma}^{u,d,ud}$. Note the non-vanishing new contribution $\hat{\sigma}_{L,R}^t$ due to the heavy top-quark exchange. One may obtain similar expressions for $\sigma_{LO}(\text{had}_1 \text{had}_2 \rightarrow W^+ V)$.

Fig. 1 shows the cross sections at the Tevatron and at the LHC with 7 TeV. The cross section $\sigma_{LO}(p\bar{p} \rightarrow W^\pm V) \sim 1$ pb can be easily achieved when $(g_L^{u,d})^2 \sim 1/50$ taking $m_V = 150$ GeV. It also can be achieved even for the top-quark exchange case but with a bit large couplings $|\tilde{g}_{L,R}^t|^2 \sim 3$ which might be constrained by the $t\bar{t}$ production cross section.

In this work, we have taken account of the constraints from the non-observation of the s -channel V production by UA2 collaboration [26]. The resonant cross section may be given by

$$\sigma_{LO}(p\bar{p} \rightarrow V) = \sum_{q=u,d} \sigma_{LO}(q\bar{q} \rightarrow V) = \frac{2\pi^2\alpha_S}{3m_V^2} \sum_{q=u,d} [(g_L^q)^2 + (g_R^q)^2] \left(\tau \frac{d\mathcal{L}^{q\bar{q}}}{d\tau} \right). \quad (7)$$

Here $\tau = m_V^2/s$ with $\sqrt{s} = 630$ GeV and

$$\tau \frac{d\mathcal{L}^{q\bar{q}}}{d\tau} = \int_\tau^1 dx \left[\frac{\tau}{x} f_p^q(x, Q_F) f_{\bar{p}}^{\bar{q}}\left(\frac{\tau}{x}, Q_F\right) + \frac{\tau}{x} f_p^{\bar{q}}(x, Q_F) f_{\bar{p}}^q\left(\frac{\tau}{x}, Q_F\right) \right]. \quad (8)$$

3 Top FB asymmetry and polarization observables

The forward-backward asymmetry A_{FB} of the top quark is one of the interesting observables related with top quark. The most recent measurement in the $t\bar{t}$ rest frame is [27]

$$A_{\text{FB}} \equiv \frac{N_t(\cos \theta \geq 0) - N_{\bar{t}}(\cos \theta \geq 0)}{N_t(\cos \theta \geq 0) + N_{\bar{t}}(\cos \theta \geq 0)} = (0.158 \pm 0.072 \pm 0.017) \quad (9)$$

with θ being the polar angle of the top quark with respect to the incoming proton in the $t\bar{t}$ rest frame. Within the SM, this asymmetry vanishes at leading order in QCD because of C symmetry. At next-to-leading order $[O(\alpha_s^3)]$, a nonzero A_{FB} can develop with the prediction $A_{\text{FB}} \sim 0.078$ [28].

Another interesting observable which is sensitive to the chiral structure of new physics affecting $q\bar{q} \rightarrow t\bar{t}$ is the top quark spin-spin correlation [29]:

$$C = \frac{\sigma(t_L\bar{t}_L + t_R\bar{t}_R) - \sigma(t_L\bar{t}_R + t_R\bar{t}_L)}{\sigma(t_L\bar{t}_L + t_R\bar{t}_R) + \sigma(t_L\bar{t}_R + t_R\bar{t}_L)}. \quad (10)$$

This quantity depends on the spin quantization axis. At leading order, the SM prediction is $C = -0.471$ for the helicity basis which we choose in this work. It is known that NLO correction to C is rather large, shifting C to -0.352 [29]. In Ref. [2], we propose a new spin-spin FB asymmetry C_{FB} defined as

$$C_{\text{FB}} \equiv C(\cos\theta \geq 0) - C(\cos\theta \leq 0), \quad (11)$$

where $C(\cos\theta \geq 0(\leq 0))$ implies that the cross sections in the numerator of Eq. (7) are obtained for the forward (backward) region: $\cos\theta \geq 0(\leq 0)$. This quantity can be measured by dividing the $t\bar{t}$ sample into the forward top and the backward top events.

In Ref. [3], we note that the NP interaction responsible for the deviation of A_{FB} from the SM prediction is parity(P)-violating. Motivated by the observation, we propose new P -odd observables:

$$\begin{aligned} D &\equiv \frac{\sigma(t_R\bar{t}_L) - \sigma(t_L\bar{t}_R)}{\sigma(t_R\bar{t}_R) + \sigma(t_L\bar{t}_L) + \sigma(t_L\bar{t}_R) + \sigma(t_R\bar{t}_L)}, \\ D_{\text{FB}} &\equiv D(\cos\hat{\theta} \geq 0) - D(\cos\hat{\theta} \leq 0) \end{aligned} \quad (12)$$

which correspond to the difference between the longitudinal polarizations of top and antitop quarks. We show the P -odd new observables provide important information on the chiral structures of NP that might be relevant to the A_{FB} .

The leading-order SM predictions for the proposed new observables are $C_{\text{FB}} = D = D_{\text{FB}} = 0$. We note that, being different from C_{FB} , the observables D and D_{FB} vanish in QCD to all orders because of P conservation. But, in the presence of NP, we still need to know how much changes will be induced by the NP+QCD corrections for quantitative studies.

4 Flavor-conserving Case

Firstly, we consider the FC couplings $g_{L,R}^t$ only for the connection to A_{FB} taking $m_V = 150$ GeV. Without losing generality, $g_L^t = g_L^u$ is taken.

With $\sigma(p\bar{p} \rightarrow W^\pm V) = K \sigma_{\text{LO}}(p\bar{p} \rightarrow W^\pm V)$ taking $K = 1.3$, one may obtain

$$\text{CDF ellipse} : (g_L^u)^2 + (g_L^d)^2 - 1.2 g_L^u g_L^d = 0.060 \left(\frac{\sigma(p\bar{p} \rightarrow W^\pm V)}{4 \text{ pb}} \right). \quad (13)$$

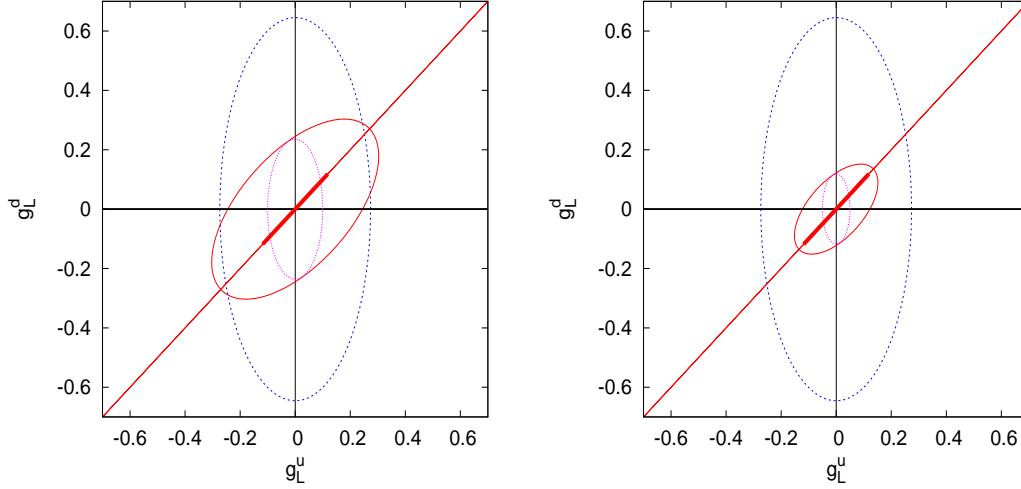


Figure 2: The **CDF** (tilted red) and **UA2** (co-axial inner and outer) ellipses on the g_L^u - g_L^d plane taking $m_V = 150$ GeV and $\sigma^{\max}(p\bar{p} \rightarrow V) = 300$ pb with $\sigma(p\bar{p} \rightarrow W^\pm V) = 4$ pb (left) and 1 pb (right). See text for explanation.

If the dijet excess reported by CDF diminishes, then the CDF ellipse should shrink accordingly, as described by the above equation. On the other hand, with $\sigma(p\bar{p} \rightarrow V) = K \sigma_{LO}(p\bar{p} \rightarrow V)$ taking $K = 1.3$, we get

$$\text{UA2 ellipse : } [(g_L^u)^2 + 0.18(g_L^d)^2] + [(g_R^u)^2 + 0.18(g_R^d)^2] \lesssim 0.075 \left(\frac{\sigma^{\max}(p\bar{p} \rightarrow V)}{300 \text{ pb}} \right). \quad (14)$$

In Fig. 2, we show the **CDF** (tilted red) and the **UA2** (co-axial inner and outer) ellipses on the g_L^u - g_L^d plane, taking $\sigma(p\bar{p} \rightarrow W^\pm V) = 4$ pb (left) and 1 pb (right) with $\sigma^{\max}(p\bar{p} \rightarrow V) = 300$ pb. For both cases, the outer **UA2** (blue) ellipses are obtained by taking $g_R^u = g_R^d = 0$ while the inner (magenta) ones are for $(g_R^u)^2 + 0.18(g_R^d)^2 = [(g_R^u)^2 + 0.18(g_R^d)^2]_{\max} \simeq 0.065$ (left) and 0.072 (right). If the sum of the right-handed couplings squared is larger than 0.065, there is no solution for the CDF dijet excess corresponding to $\sigma(WV) = 4$ pb. When the sum increases further, the **UA2** bound becomes stronger. And, if it is larger than 0.072, the left-handed couplings are too small to achieve even $\sigma(WV) = 1$ pb. Therefore, $(g_R^u)^2 + 0.18(g_R^d)^2 \lesssim 0.072$ is required to accommodate $\sigma(WV) = 1 - 4$ pb.

The thick solid (red) straight line along $g_L^u = g_L^d$ in Fig. 2 presents the case of the leptophobic Z' model in a particular type of E_6 model [30], where the couplings of Z' to the SM quarks are related as $g_L^u = g_L^d = g_R^u/2 = -g_R^d$. We find the leptophobic model gives at most $\sigma(p\bar{p} \rightarrow W^\pm V) \simeq 0.77$ pb, which is rather small compared with the presumed cross section of 1 – 4 pb.

When $g_R^u = g_R^d = 0$, we find the solutions, represented by the points on the tilted **CDF** ellipse inside of the outer **UA2** one, always result in $A_{\text{FB}} < A_{\text{FB}}^{\text{SM}}$, which is not satisfactory. Therefore, one cannot explain both the top FB asymmetry and the CDF dijet excess in terms of FC: $g_L^u = g_L^d \neq 0$ and $g_R^u = g_R^d = 0$.

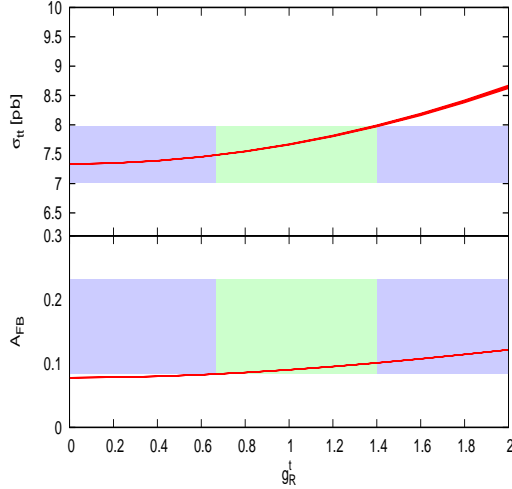


Figure 3: The $t\bar{t}$ production cross section and the forward-backward asymmetry are shown as functions of the coupling g_R^t in the FC case taking $m_V = 150$ GeV and $(g_R^u)^2 + 0.18(g_R^d)^2 = [(g_R^u)^2 + 0.18(g_R^d)^2]_{\max} \simeq 0.065$ with g_R^u varying from 0 to $(g_R^u)_{\max} \sim 0.25$. The left-handed couplings are given by $(g_L^u, g_L^d) \simeq (\pm 0.029, \mp 0.23)$ and we have taken $g_L^t = g_L^u$. The two horizontal bands show the experimental 1- σ regions, $\sigma_{t\bar{t}} = 7.50 \pm 0.48$ pb and $A_{\text{FB}} = 0.158 \pm 0.074$ [1]. The vertical bands show the 1- σ allowed region for the coupling g_R^t .

On the other hand, when the sum $(g_R^u)^2 + 0.18(g_R^d)^2$ takes its maximum value $\simeq 0.065$ with $\sigma(p\bar{p} \rightarrow W^\pm V) = 4$ pb, we have the solutions $(g_L^u, g_L^d) \simeq (\pm 0.029, \mp 0.23)$ given by the two overlapping points of the **CDF** and inner **UA2** ellipses, see the left frame of Fig. 2. In this case, we find the simultaneous solutions to the CDF dijet excess and the large A_{FB} are possible if $0.67 \lesssim g_R^t \lesssim 1.4$, see Fig. 3. We observe this is quite large compared to $(g_R^u)_{\max} \sim 0.25$. Note that the coupling $g_R^t \sim 1.4$ is still small enough for perturbation, since $(g_s g_R^t)^2 / 4\pi \sim 0.2$.

The $t\bar{t}$ production cross section and the forward-backward asymmetry are not much affected by taking the smaller $\sigma(p\bar{p} \rightarrow W^\pm V) = 1$ pb. This is because the NP contribution to the top-quark pair production is dominated by the right-handed couplings and their squared sum increases only by ~ 10 %.

5 Flavor-violating Case

Secondly, taking $m_V = 150$ GeV again, we consider the right-handed FV coupling \tilde{g}_R^t with $\tilde{g}_L^t = g_R^t = 0$ for the connection to A_{FB} while keeping the left-handed FC couplings g_L^t .

In this case the **UA2** ellipses remain the same but the **CDF** one has an additional term:

$$\text{CDF ellipse} : (g_L^u)^2 + (g_L^d)^2 - 1.2 g_L^u g_L^d + 0.0070 |\tilde{g}_R^t|^2 = 0.060 \left(\frac{\sigma(p\bar{p} \rightarrow W^\pm V)}{4 \text{ pb}} \right). \quad (15)$$

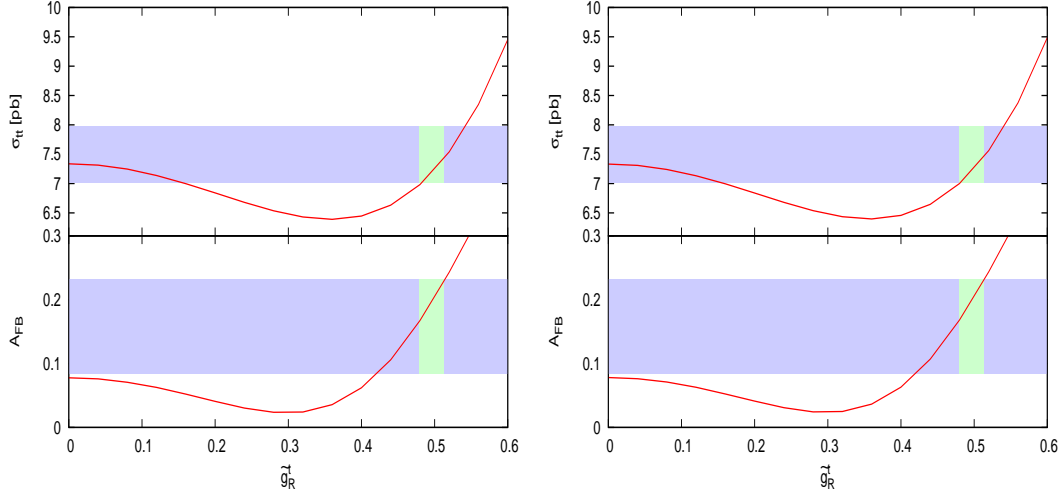


Figure 4: The $t\bar{t}$ production cross section and the forward-backward asymmetry in the FV case as functions the coupling \tilde{g}_R^t taking $m_V = 150$ GeV. Left: The other couplings are given by Eqs. (16) and (18) with $\omega_L = -1$ and $g_R^t = \tilde{g}_L^t = 0$. Right: The only non-vanishing coupling other than \tilde{g}_R^t is g_L^u which takes a more or less fixed value of about $0.24\sqrt{\sigma(p\bar{p} \rightarrow W^\pm V)/4\text{ pb}}$. The vertical bands show the 1- σ allowed region for the coupling \tilde{g}_R^t .

To reduce the number of independent couplings, we assume the relations

$$g_L^u = g_L^t = g_L^d/\omega_L, \quad g_R^u = g_R^d \equiv \omega_R g_L^u, \quad (16)$$

with $\omega_L^2 = 1$. Under the assumption, by combining the **UA2** and **CDF** conditions, one may obtain an inequality

$$\sigma(p\bar{p} \rightarrow W^\pm V)/\text{pb} \lesssim (2 - 1.2\omega_L) \left[\frac{4.2}{1 + \omega_R^2} \left(\frac{\sigma^{\max}(p\bar{p} \rightarrow V)}{300 \text{ pb}} \right) \right] + 0.47 |\tilde{g}_R^t|^2. \quad (17)$$

We observe the cross section becomes smaller with the choice $\omega_L = +1$ as ω_R grows.

Taking $\omega_L = -1$ and $\sigma^{\max}(p\bar{p} \rightarrow V) = 300$ pb, we have

$$g_L^u = \sqrt{\frac{\left[0.060 \left(\frac{\sigma(p\bar{p} \rightarrow W^\pm V)}{4 \text{ pb}} \right) - 0.0070 |\tilde{g}_R^t|^2 \right]}{3.2}}; \quad g_R^u = \sqrt{\frac{0.075 - 1.2 (g_L^u)^2}{1.2}} \quad (18)$$

where g_R^u is fixed to saturate the **UA2** bound. When $\sigma(p\bar{p} \rightarrow W^\pm V) = 4$ pb, we find the simultaneous solutions to the CDF dijet excess and the large A_{FB} are possible if $0.48 \lesssim \tilde{g}_R^t \lesssim 0.51$, see the left frame of Fig. 4, giving $g_L^u \sim 0.13$ and $g_R^u \sim 0.21$. When $\sigma(p\bar{p} \rightarrow W^\pm V) = 1$ pb, while we have the smaller coupling $g_L^u \sim 0.064$ with $g_R^u \sim 0.24$, we find that the range of \tilde{g}_R^t for the simultaneous solutions almost remains the same since the NP contribution to the top-quark production is dominated by the t -channel diagram which depends only on the coupling \tilde{g}_R^t .

Taking $\omega_L = +1$ and $\sigma^{\max}(p\bar{p} \rightarrow V) = 300$ pb, we find $\sigma(p\bar{p} \rightarrow W^\pm V)$ can not be larger than $\sim (3.4/(1 + \omega_R^2) + 0.47|\tilde{g}_R^t|^2)$ pb, see Eq. (17), in which we find $|\tilde{g}_R^t| \lesssim 0.5$ constrained by the $t\bar{t}$ production cross section. Therefore, the right-handed couplings are constrained by $\omega_R^2 \lesssim 2.8$ in order to have $\sigma(p\bar{p} \rightarrow W^\pm V) \gtrsim 1$ pb.

Actually, in the FV case, we find that it is possible to explain the CDF dijet excess and the large A_{FB} simultaneously only with the two couplings g_L^u and \tilde{g}_R^t by noting that the s -channel contribution to the $t\bar{t}$ production is negligible under the assumption $g_L^t = g_L^u$ (16). Only with g_L^u and \tilde{g}_R^t non-vanishing, we observe that g_L^u takes a more or less fixed value of about $0.24\sqrt{\sigma(p\bar{p} \rightarrow W^\pm V)/4\text{ pb}}$ and \tilde{g}_R^t should take values between 0.48 and 0.51, see the right frame of Fig. 4 which does not show any visible difference from the left frame reflecting the negligible s -channel contribution via the FC coupling g_L^t .

Finally, in the left frame of Fig. 5, we show A_{FB} in the low and high invariant mass regions of the top-quark pair taking the FC point with $g_R^t = 1.4$ (triangle) from Fig. 3 and the FV points with $\tilde{g}_R^t = 0.51$ (square) from Fig. 4. We observe that the FV case leads to the consistent results with the current measurement of the mass dependent FB asymmetry [1]. For the FC case, we have somewhat lower A_{FB} than the current data and the future analysis with more data could tell more definitely whether the FC case is viable or not.

In the middle and right frames of Fig. 5, we show our predictions for the polarization observables C and C_{FB} and D and D_{FB} , respectively, in the $1\text{-}\sigma$ allowed regions for the FC coupling g_R^t and FV coupling \tilde{g}_R^t . We find $-C$ and $-C_{\text{FB}}$ can be as large as 0.62 and 0.2, respectively, in the FV case. On the other hand, D and D_{FB} can be as large as 0.18 and 0.13, respectively. The SM prediction is $C = -0.352$ at NLO and, for other observables, the leading-order SM predictions are $C_{\text{FB}} = D = D_{\text{FB}} = 0$. To our best knowledge, there are no available calculations of the latter including QCD corrections which renders it difficult to make a decisive model discrimination at the current stage. Implementing QCD corrections to these observables deserves more theoretical works in the future. With more data accumulated at the Tevatron and LHC, these new observables of C_{FB} , D , and D_{FB} can give useful and independent information on NP scenarios.

Before we close this section we comment on the *direct* constraint on the flavor-changing coupling on \tilde{g}_R^t obtained by the CMS Collaboration in search for same-sign top-quark pair production at the LHC [31]. The constraint is $\tilde{g}_R^t \lesssim 0.4$ when $m_V = 150$ GeV at the 95 % confidence level. Taking this limit seriously, our FV solution for A_{FB} with $\tilde{g}_R^t \sim 0.5$ is not viable.

6 Conclusions

In this work, we have introduced a neutral color-singlet vector boson V_μ in order to explain the CDF dijet excess. We find that each of the exchanges of the left-handed u and d quarks can easily accommodate $\sigma(p\bar{p} \rightarrow W^\pm V) \sim 1 - 4$ pb, if $m_V = 150$ GeV with $g_L^u, g_L^d \sim 0.12 - 0.24$. When $g_L^u = -g_L^d \sim 0.064 - 0.13$, we may also have the $1 - 4$ pb

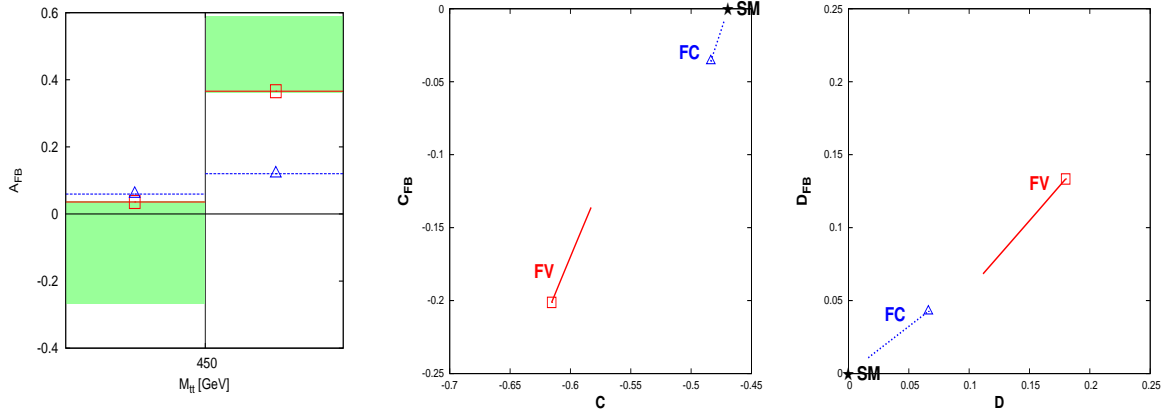


Figure 5: *Left: The $M_{t\bar{t}}$ dependent A_{FB} for the FC point with $g_R^t = 1.4$ (triangle) and the FV points with $\tilde{g}_R^t = 0.51$ (square). Middle and Right: The polarization observables C and C_{FB} (middle) and D and D_{FB} (right) in the $1\text{-}\sigma$ allowed regions for the FC and FV couplings: $0.67 \lesssim g_R^t \lesssim 1.4$ and $0.48 \lesssim \tilde{g}_R^t \lesssim 0.51$. The leading order SM predictions are denoted by stars.*

cross section. On the other hand, with $g_L^u = +g_L^d$, the cross section $\sigma(p\bar{p} \rightarrow W^\pm V)$ becomes smaller due to the destructive interference between the t - and u -channel diagrams combined with the UA2 bounds and the right-handed couplings are constrained by $(g_R^{u,d})^2 \lesssim 2.8 (g_L^{u,d})^2$ in order to have $\sigma(p\bar{p} \rightarrow W^\pm V) \gtrsim 1$ pb.

Towards the simultaneous explanation for both the top FB asymmetry and the dijet resonance, we consider the FC and FV couplings of the top quarks to the same vector boson relevant to the CDF dijet excess. In the FC case, we find the two puzzles can be resolved with sizeable right-handed couplings of $g_R^u \sim 0.25$ or $g_R^d \sim 0.6$ together with $0.67 \lesssim g_R^t \lesssim 1.4$. This solution is almost independent of $\sigma(p\bar{p} \rightarrow W^\pm V)$ because the NP contribution to the top-quark pair production is dominated by the right-handed couplings. In the FV case, the coupling $\tilde{g}_R^t \sim 0.5$ may provide the simultaneous solutions with $g_L^u = -g_L^d \sim 0.064 - 0.13$ or $g_L^u \sim 0.12 - 0.24$ to accommodate $1 \text{ pb} \lesssim \sigma(p\bar{p} \rightarrow W^\pm V) \lesssim 4$ pb. Again, we observe that the solution for A_{FB} with $\tilde{g}_R^t \sim 0.5$ is almost independent of $\sigma(p\bar{p} \rightarrow W^\pm V)$ because the NP contribution to the top-quark production is dominated by the t -channel diagram which depends only on the coupling \tilde{g}_R^t .

From Fig. 5, we observe that the FC and FV cases can be distinguished in the mass dependence of the top FB asymmetry if more data is accumulated and analyzed. However one can have additional handles to diagnose the new physics structure using the FB spin-spin correlation or longitudinal top polarization, as suggested in Refs. [2, 3]. It is highly desirable to measure and extract these observables from the current data set obtained at the Tevatron.

Having identified the coupling structures that are needed to accommodate both the CDF dijet excess and the top FB asymmetry, the next important question would be to construct a realistic model with such a neutral vector boson. Since the couplings are flavor dependent and might have a large FV $u_R - t_R$ coupling, it might be challenging to build

such a model. (See, for example, Refs. [14, 18, 32, 33] for the attempts in this direction.)

Independently of the model building, a light vector boson ($\lesssim 200$ GeV) coupling only to quarks has been elusive at colliders. The Wjj channel at hadron colliders is one of the best to probe such light leptophobic gauge boson. It remains to be seen if the further data analysis at the Tevatron and the LHC could give any hint for or strong constraint on such a leptophobic gauge boson.

There are some more phenomenological issues: *(i)* the LHC signatures of the FC and FV solutions found in this work *, *(ii)* the production of the NP particle (V) associated with γ , W^\pm , Z , and V itself at hadron colliders, *(iii)* the single top and same-sign top pair productions, *(iv)* other possibilities with neutral and charged NP particles of color-singlet/octet scalar and vector bosons, *(v)* model discrimination by use of the top-quark polarizations, etc. We address these issues in future publications.

Acknowledgements

The work by PK is supported in part by Korea National Research Foundation through Korea Neutrino Research Center (KNRC) at Seoul National University.

References

- [1] T. Aaltonen *et al.* [CDF Collaboration], arXiv:1101.0034 [hep-ex].
- [2] D. W. Jung, P. Ko, J. S. Lee and S. h. Nam, Phys. Lett. B **691**, 238 (2010) [arXiv:0912.1105 [hep-ph]].
- [3] D. -W. Jung, P. Ko, J. S. Lee, Phys. Lett. **B701** (2011) 248-254. [arXiv:1011.5976 [hep-ph]].
- [4] T. Aaltonen *et al.* [CDF Collaboration], Phys. Rev. Lett. **106** (2011) 171801. [arXiv:1104.0699 [hep-ex]].
- [5] M. R. Buckley, D. Hooper, J. Kopp and E. Neil, arXiv:1103.6035 [hep-ph].
- [6] F. Yu, arXiv:1104.0243 [hep-ph].
- [7] E. J. Eichten, K. Lane and A. Martin, arXiv:1104.0976 [hep-ph].
- [8] C. Kilic and S. Thomas, arXiv:1104.1002 [hep-ph].
- [9] K. Cheung and J. Song, arXiv:1104.1375 [hep-ph].
- [10] J. A. Aguilar-Saavedra and M. Perez-Victoria, arXiv:1104.1385 [hep-ph].

* At the LHC with 7 TeV, taking $m_V = 150$ GeV, we find that $\sigma_{LO}(pp \rightarrow W^\pm V) \sim 22$ pb and 24 pb for the FC and FV cases, respectively, see the right frame of Fig. 1.

- [11] X. G. He and B. Q. Ma, arXiv:1104.1894 [hep-ph].
- [12] X. P. Wang, Y. K. Wang, B. Xiao, J. Xu and S. h. Zhu, arXiv:1104.1917 [hep-ph].
- [13] R. Sato, S. Shirai and K. Yonekura, arXiv:1104.2014 [hep-ph].
- [14] A. E. Nelson, T. Okui and T. S. Roy, arXiv:1104.2030 [hep-ph].
- [15] L. A. Anchordoqui, H. Goldberg, X. Huang, D. Lust and T. R. Taylor, arXiv:1104.2302 [hep-ph].
- [16] B. A. Dobrescu and G. Z. Krnjaic, arXiv:1104.2893 [hep-ph].
- [17] Z. Fodor, K. Holland, J. Kuti, D. Nogradi and C. Schroeder, arXiv:1104.3124 [hep-lat].
- [18] S. Jung, A. Pierce and J. D. Wells, arXiv:1104.3139 [hep-ph].
- [19] M. Buckley, P. F. Perez, D. Hooper and E. Neil, arXiv:1104.3145 [hep-ph].
- [20] G. Zhu, arXiv:1104.3227 [hep-ph].
- [21] Z. Sullivan and A. Menon, arXiv:1104.3790 [hep-ph].
- [22] P. Ko, Y. Omura and C. Yu, arXiv:1104.4066 [hep-ph].
- [23] T. Plehn and M. Takeuchi, arXiv:1104.4087 [hep-ph].
- [24] V. M. Abazov [D0 Collaboration], Phys. Rev. Lett. **107** (2011) 011804. [arXiv:1106.1921 [hep-ex]].
- [25] R. W. Brown, D. Sahdev, K. O. Mikaelian, Phys. Rev. **D20** (1979) 1164.
- [26] J. Alitti *et al.* [UA2 Collaboration], Z. Phys. **C49** (1991) 17-28.
- [27] Talk by E. Shabalina, 22nd Rencontres de Blois, July 15-20, 2010, Blois, France.
- [28] J. H. Kuhn and G. Rodrigo, Phys. Rev. Lett. **81**, 49 (1998); J. H. Kuhn and G. Rodrigo, Phys. Rev. D **59**, 054017 (1999); O. Antunano, J. H. Kuhn and G. Rodrigo, Phys. Rev. D **77**, 014003 (2008).
- [29] G. Mahlon and S. J. Parke, Phys. Rev. D **53**, 4886 (1996); T. Stelzer and S. Willenbrock, Phys. Lett. B **374**, 169 (1996); W. Bernreuther, A. Brandenburg, Z. G. Si and P. Uwer, Nucl. Phys. B **690**, 81 (2004).
- [30] D. London, J. L. Rosner, Phys. Rev. **D34** (1986) 1530; J. L. Rosner, Phys. Lett. **B387** (1996) 113-117. [hep-ph/9607207].
- [31] S. Chatrchyan *et al.* [CMS Collaboration], [arXiv:1106.2142 [hep-ex]].
- [32] S. Jung, A. Pierce and J. D. Wells, arXiv:1103.4835 [hep-ph].
- [33] P. Ko, Y. Omura, C. Yu, arXiv:1108.0350 [hep-ph].